Hybrid Beamforming With Variable RF Attenuator for Multi-User mmWave Systems

Jungjoo Lee, Taeseok Oh, Jihwan Moon, Changick Song, *Senior Member, IEEE*, Byeongsi Lee, and Inkyu Lee, *Fellow, IEEE*

***Abstract*—In this paper, we propose a novel hybrid beamforming design algorithm in multi-user massive multiple-input-multiple-output millimeter-wave channels. In the proposed structure, we employ variable radio frequency attenuators at each phase shifter which flexibly controls the transmit signal amplitude to achieve the performance of fully digital (FD) precoders. We formulate a power loss minimization problem which can be easily solved via the alternating optimization process. Simulation results demonstrate that the proposed architecture achieves the same performance as the FD scheme with the reduced number of radio frequency chains and the proposed scheme exhibits a 37.4% power gain over conventional methods.**

***Index Terms*—Hybrid beamforming, variable RF attenuator, millimeter wave systems.**

I. Introduction

For the past decades, communication technologies have been developed to improve spectral efficiency (SE). Existing Long-Term Evolution (LTE) systems have experienced difficulties in meeting ever-increasing data traffic demand while facing the scarcity issue of available bandwidth resources. In response to this, recently launched fifth generation (5G) systems now adopt millimeter- wave (mmWave) frequency bands, in which a much broader bandwidth can be exploited. The mmWave transmission systems allow designing a massive antenna array, which is composed of a large number of antenna elements, in a small form factor [1], [2].

When employing the massive antenna array, a fully digital (FD) beamforming approach induces high implementation cost [3], since a radio frequency (RF) chain must be installed at every antenna elements. To solve this cost issue, hybrid beamforming (HBF) techniques [4] that separately design a baseband (BB) precoder and a RF precoder has been studied, which reduces the required number of RF chains. However, there exists a noticeable performance degradation compared to the FD architecture due to constant power constraint imposed at phase shifters of the RF precoder [4]–[10]. Some analytical results in [3] and [11] have revealed that the performance gap between the FD scheme and the HBF can be negligibly small when the number of RF chains is at least twice that of data streams. However, such approaches still require a large number of RF chains in multi-user massive multiple-input-multiple-output (MIMO) environments.

Recently, it has been shown in [3] and [12] that the HBF can approach the performance of the FD scheme with the smaller number of RF chains when the HBF is followed by a set of variable gain amplifiers (VGA). The VGA based hybrid precoding scheme was proposed in [13] for mmWave multi-user MIMO systems. However, it has been pointed out in [14], [15] that the VGAs show poor performance in terms of stability, power dissipation, and amplitude-scaling speed, which are utmost important requirements for wideband applications. Instead, a variable RF attenuator (VRA) which only changes the amplitude of the analog signal can be a more attractive solution. Nevertheless, a HBF design based on the variable RF attenuator has not yet been discussed in the literature.

In this paper, we investigate a novel HBF design in which a VRA is appended at each phase shifter. Contrary to the conventional HBF designs [4]–[12], the VRAs can flexibly control the RF signal amplitudes which enables us to derive more effective precoders. One drawback of the VRA is the radiation power loss at the RF front ends due to signal attenuation. To reduce such an effect, we first define an attenuation loss minimization problem which is generally non-convex. Then we reformulate the problem such that it can be efficiently solved by an alternating optimization process. Finally, we perform numerical simulations to validate the efficacy of our proposed algorithm. Simulation results demonstrate that the proposed architecture achieves the same SE as the FD scheme with much reduced RF chains at the expense of a slight attenuation loss. Also, the proposed scheme has at least 37.4% gain over conventional HBF methods in terms of the attenuation loss.

Throughout this paper, the following notations are used. Uppercase boldface, lowercase boldface and normal letters represent a matrix, a vector and a scalar number, respectively. The notation $\mathbf{A}^{(i,j)}$ and $\|\mathbf{A}\|_F$ denote the (i,j)-th element and Frobenius norm of a matrix $\mathbf{A}$, respectively. The operators $\circ$, $(\cdot)^T$ and $(\cdot)^H$ indicate Hadamard product, transpose and conjugate transpose, respectively. Further, $|a|$ stands for the amplitude of a complex number a.

II. System Model

We consider a multi-user MIMO mmWave system where a base station (BS) with $N_{\rm BS}$ antennas and $M_{\rm BS}$ RF chains supports K user equipments (UEs) with $N_{\rm UE}$ antennas and $M_{\rm UE}$ RF chains. To guarantee the effectiveness of the HBF system, the number of RF chains is constrained by $M_{\rm BS} < N_{\rm BS}$ and $M_{\rm UE} < N_{\rm UE}$. Each UE receives $N_{\rm s}$ data streams so that a total of KN_s data streams are handled by the BS. Also, we assume a full data load situation, i.e., $M_{\rm BS} = KN_s$ and $M_{\rm UE} = N_s$. The proposed HBF structure with variable RF attenuators is illustrated in Fig. 1.

Let us denote $\mathbf{F}_{\rm A} \in \mathbb{R}^{N_{\rm BS}\times M_{\rm BS}}$ and $\mathbf{W}_{{\rm A},k} \in \mathbb{R}^{N_{\rm UE}\times M_{\rm UE}}$ as the RF attenuator matrices for a transmitter and a receiver, respectively, such that $|\mathbf{F}_{\rm A}^{(i,j)}| \leq 1$ and $|\mathbf{W}_{{\rm A},k}^{(i,j)}| \leq 1$ for $\forall\, i,j,k$. Then the effective RF precoder $\mathbf{F}_{\rm RFA} \in \mathbb{C}^{N_{\rm BS}\times M_{\rm BS}}$ at the BS and the RF combiner $\mathbf{W}_{{\rm RFA},k} \in \mathbb{C}^{N_{\rm UE}\times M_{\rm UE}}$ at the k-th UE are expressed as

$$\mathbf{F}_{\rm RFA} \triangleq \mathbf{F}_{\rm RF} \circ \mathbf{F}_{\rm A}, \tag{1}$$

$$\mathbf{W}_{{\rm RFA},k} \triangleq \mathbf{W}_{{\rm RF},k} \circ \mathbf{W}_{{\rm A},k}, \tag{2}$$

where $\mathbf{F}_{\rm RF} \in \mathbb{C}^{N_{\rm BS}\times M_{\rm BS}}$ and $\mathbf{W}_{{\rm RF},k} \in \mathbb{C}^{N_{\rm UE}\times M_{\rm UE}}$ represent the RF precoder and the RF combiner of the traditional HBF, respectively.

Manuscript received November 12, 2019; revised March 12, 2020; accepted May 13, 2020. Date of publication May 21, 2020; date of current version August 13, 2020. This work was supported by the National Research Foundation through the Ministry of Science, ICT, and Future Planning (MSIP), Korean Government under Grant 2017R1A2B3012316. The review of this article was coordinated by Dr. H. Lin. *(Corresponding author: Inkyu Lee.)*

Jungjoo Lee, Jihwan Moon, and Inkyu Lee are with the School of Electrical Engineering, Korea University, Seoul 02841, South Korea (e-mail: dlwjdwn888@gmail.com; anschino@korea.ac.kr; inkyu@korea.ac.kr).

Taeseok Oh is with the Agency for Defense Development, Daejeon 34186, South Korea (e-mail: taeseok@add.re.kr).

Changick Song is with the Department of Electronic Engineering, Korea National University of Transportation, Chungju 27469, South Korea (e-mail: c.song@ut.ac.kr).

Byeongsi Lee is with the Samsung Electronics, Suwon 443-743, South Korea (e-mail: byeongsi@samsung.com).

Digital Object Identifier 10.1109/TVT.2020.2996193

0018-9545 © 2020 IEEE. Personal use is permitted, but republication/redistribution requires IEEE permission.
See https://www.ieee.org/publications/rights/index.html for more information.

Authorized licensed use limited to: Korea University. Downloaded on August 18,2020 at 09:08:21 UTC from IEEE Xplore. Restrictions apply.

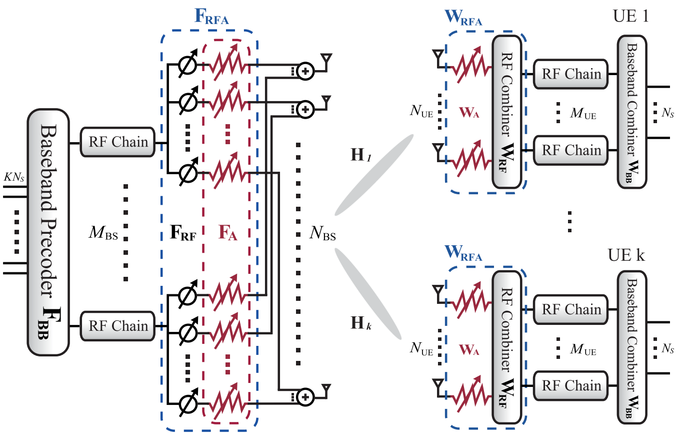

Fig. 1. Proposed hybrid beamforming structure with variable RF attenuator in multi-user massive MIMO systems.

As a result, we obtain the received signal at the k-th UE as

$$\mathbf{y}_k = \mathbf{H}_k \mathbf{F}_{\mathrm{RFA}} \mathbf{F}_{\mathrm{BB}} \mathbf{s} + \mathbf{n}_k, \tag{3}$$

where $\mathbf{H}_k$ denotes the channel matrix between the BS and the k-th UE. $\mathbf{F}_{\mathrm{BB}}$ stands for $\mathbf{F}_{\mathrm{BB}} \triangleq \left[\mathbf{F}_{\mathrm{BB},1}, \mathbf{F}_{\mathrm{BB},2}, \ldots, \mathbf{F}_{\mathrm{BB},K}\right]$ with $\mathbf{F}_{\mathrm{BB},k} \in \mathbb{C}^{M_{\mathrm{BS}} \times N_{\mathrm{s}}}$ being the precoding matrix for the k-th UE, $\mathbf{s} \triangleq \left[\mathbf{s}_1^T, \mathbf{s}_2^T, \ldots, \mathbf{s}_K^T\right]^T \in \mathbb{C}^{KN_{\mathrm{s}} \times 1}$ is the transmitted symbol vector of data streams, $\mathbf{s}_k \in \mathbb{C}^{N_{\mathrm{s}} \times 1}$ represents the symbol vector for the k-th UE, and $\mathbf{n}_k \in \mathbb{C}^{N_{\mathrm{UE}} \times 1}$ indicates the independent identically distributed (i.i.d.) additive complex Gaussian noise vector at the k-th UE. Note that $\mathbf{F}_{\mathrm{BB}} \in \mathbb{C}^{M_{\mathrm{BS}} \times M_{\mathrm{BS}}}$ is invertable since a full data load is assumed. Also, we adopt a general mmWave channel model which captures the highly directional propagation property [4].

Next, the k-th UE combines its received signals by the RF attenuator $\mathbf{W}_{\mathrm{A},k}$, the RF combiners $\mathbf{W}_{\mathrm{RF},k}$ and the BB combiner $\mathbf{W}_{\mathrm{BB},k} \in \mathbb{C}^{M_{\mathrm{UE}} \times N_{\mathrm{s}}}$. The resultant signal at the k-th UE becomes

$$\begin{aligned}\widetilde{\mathbf{y}}_k &= \mathbf{W}_{\mathrm{BB},k}^H \mathbf{W}_{\mathrm{RFA},k}^H \mathbf{H}_k \mathbf{F}_{\mathrm{RFA}} \mathbf{F}_{\mathrm{BB},k}\, \mathbf{s}_k \\ &\quad + \sum_{i=1, i \neq k}^{K} \mathbf{W}_{\mathrm{BB},k}^H \mathbf{W}_{\mathrm{RFA},k}^H \mathbf{H}_k \mathbf{F}_{\mathrm{RFA}} \mathbf{F}_{\mathrm{BB},i}\, \mathbf{s}_i \\ &\quad + \mathbf{W}_{\mathrm{BB},k}^H \mathbf{W}_{\mathrm{RFA},k}^H\, \mathbf{n}_k, k = 1, 2, \ldots, K. \end{aligned} \tag{4}$$

Note that $\mathbf{W}_{\mathrm{RFA},k}$ reduces the noise power as well as the signal power equally, and thus the received signal-to-noise ratio remains unchanged.

From (4), the sum rate can be computed as

$$\begin{aligned} &R(\mathbf{F}_{\mathrm{RFA}}, \mathbf{F}_{\mathrm{BB}}, \mathbf{W}_{\mathrm{RFA},k}, \mathbf{W}_{\mathrm{BB},k}) \\ &= \sum_{k=1}^{K} \log_2(|\mathbf{I}_{N_{\mathrm{s}}} + \mathbf{R}_{\mathrm{c}}^{-1} \mathbf{W}_{\mathrm{BB},k}^H \mathbf{W}_{\mathrm{RFA},k}^H \mathbf{H}_k \mathbf{F}_{\mathrm{RFA}} \mathbf{F}_{\mathrm{BB},k} \\ &\qquad \times \mathbf{F}_{\mathrm{BB},k}^H \mathbf{F}_{\mathrm{RFA}}^H \mathbf{H}_k^H \mathbf{W}_{\mathrm{RFA},k} \mathbf{W}_{\mathrm{BB},k}|), \end{aligned} \tag{5}$$

where $\mathbf{R}_{\mathrm{c}} \triangleq \sum_{i=1, i\neq k}^{K} \mathbf{W}_{\mathrm{BB},k}^H \mathbf{W}_{\mathrm{RFA},k}^H \mathbf{H}_k \mathbf{F}_{\mathrm{RFA}} \mathbf{F}_{\mathrm{BB},i} \times \mathbf{F}_{\mathrm{BB},i}^H \mathbf{F}_{\mathrm{RFA}}^H \mathbf{H}_k^H \mathbf{W}_{\mathrm{RFA},k} \mathbf{W}_{\mathrm{BB},k} + \sigma^2 \mathbf{W}_{\mathrm{BB},k}^H \mathbf{W}_{\mathrm{RFA},k}^H \mathbf{W}_{\mathrm{RFA},k} \mathbf{W}_{\mathrm{BB},k}$. Here, the effective RF precoder and RF combiner are constrained by

$$|\mathbf{F}_{\mathrm{RFA}}^{(i,j)}| \leq \frac{1}{\sqrt{N_{\mathrm{BS}}}}, \ \forall\, i, j, \tag{6}$$

$$|\mathbf{W}_{\mathrm{RFA},k}^{(i,j)}| \leq \frac{1}{\sqrt{N_{\mathrm{UE}}}}, \ \forall\, i, j, k, \tag{7}$$

$$\|\mathbf{F}_{\mathrm{RFA}} \mathbf{F}_{\mathrm{BB}}\|_F^2 \leq P_{\mathrm{rad}}, \tag{8}$$

where P_{rad} indicates the radiated power at the transmitter. The constraints in (6) and (7) come from the fact that the VRAs in the effective RF precoder $\mathbf{F}_{\mathrm{RFA}}$ and the combiners $\mathbf{W}_{\mathrm{RFA},k}$ serve to reduce the amplitude of each phase shifter output, and (8) accounts for the radiated power constraint at the BS.

III. Hybrid Beamforming With Attenuation Loss Minimization

In this section, we first show that the proposed HBF architecture with the VRA can achieve the performance of the FD precoding systems. Then, we suggest a new HBF design algorithm that minimizes the attenuation loss.

A. Effects of Variable RF Attenuators

In the proposed HBF structure with variable RF attenuators, each element of the effective precoder $\mathbf{F}_{\mathrm{RFA}}$ can have magnitude within $[0, \frac{1}{\sqrt{N_{\mathrm{BS}}}}]$. This means that the effective precoder $\mathbf{F}_{\mathrm{RFA}}$ is free from the constant magnitude constraint, which is normally imposed to conventional HBF methods. Moreover, the maximum rank of $\mathbf{F}_{\mathrm{RFA}}\mathbf{F}_{\mathrm{BB}}$ equals M_{BS} which is identical to that of $\mathbf{F}_{\mathrm{FD}}$, since $\mathbf{F}_{\mathrm{BB}}$ is an $M_{\mathrm{BS}} \times M_{\mathrm{BS}}$ unconstrained square matrix under the full data load assumption. This demonstrates that any FD precoder $\mathbf{F}_{\mathrm{FD}}$ can be expressed as a multiplication of the effective RF precoder $\mathbf{F}_{\mathrm{RFA}}$ and the unconstrained weight matrix $\mathbf{F}_{\mathrm{BB}}$. Note that the same argument can be made for $\mathbf{W}_{\mathrm{FD},k} = \mathbf{W}_{\mathrm{RFA},k}\mathbf{W}_{\mathrm{BB},k}$ without loss of generality. Therefore, unlike conventional HBF methods, our proposed structure with variable RF attenuators can reproduce the FD transceiver $\mathbf{F}_{\mathrm{FD}}$ and the receiver $\mathbf{W}_{\mathrm{FD},k}$, and thus provides the same performance as the FD scheme with the reduced number of RF chains. To compensate for the attenuation loss caused by the VRA, more power may be needed at the pre-attenuator stage. To minimize such a loss, we propose an efficient HBF design algorithm which minimizes the attenuation loss at the transmitter in the next subsection.

B. Proposed HBF Design With Attenuation Loss Minimization

Let us denote $P_{\mathrm{pre\_att}}$ and $P_{\mathrm{post\_att}}$ as the transmitter power before and after the attenuator, respectively. Then, we can define the attenuation loss P_{A} under the assumption $\mathbf{F}_{\mathrm{RFA}}\mathbf{F}_{\mathrm{BB}} = \mathbf{F}_{\mathrm{FD}}$ as

$$\begin{aligned} P_{\mathrm{A}} = P_{\mathrm{pre\_att}} - P_{\mathrm{post\_att}} &= \|\mathbf{F}_{\mathrm{RF}}\mathbf{F}_{\mathrm{BB}}\|_F^2 - \|\mathbf{F}_{\mathrm{RFA}}\mathbf{F}_{\mathrm{BB}}\|_F^2 \\ &= \|\mathbf{F}_{\mathrm{RF}}\mathbf{F}_{\mathrm{BB}}\|_F^2 - \|\mathbf{F}_{\mathrm{FD}}\|_F^2. \end{aligned} \tag{9}$$

Thus, the objective function that minimizes the attenuation loss P_{A} is simple as it is essentially equivalent to minimizing $\|\mathbf{F}_{\mathrm{RF}}\mathbf{F}_{\mathrm{BB}}\|_F^2$ since $\mathbf{F}_{\mathrm{FD}}$ is fixed for given channel state information. However, it is still not easy to handle constraints (6) and (7) due to the Hadamard product.

To resolve such an issue, let us introduce a new attenuator loss matrix $\mathbf{F}_{\mathrm{L}} \in \mathbb{C}^{N_{\mathrm{BS}} \times M_{\mathrm{BS}}}$ as

$$\mathbf{F}_{\mathrm{L}} = \mathbf{F}_{\mathrm{RF}} - \mathbf{F}_{\mathrm{RFA}}, \tag{10}$$

where the phase of $\mathbf{F}_{\mathrm{RFA}}$, $\mathbf{F}_{\mathrm{RF}}$, and $\mathbf{F}_{\mathrm{L}}$ should remain the same, i.e., $\angle\, \mathbf{F}_{\mathrm{RFA}}^{(i,j)} = \angle\, \mathbf{F}_{\mathrm{RF}}^{(i,j)} = \angle\, \mathbf{F}_{\mathrm{L}}^{(i,j)}$, for all i and j because the attenuator

Authorized licensed use limited to: Korea University. Downloaded on August 18,2020 at 09:08:21 UTC from IEEE Xplore. Restrictions apply.

coefficient matrix $\mathbf{F}_{\text{RFA}}$ controls the amplitude only. Also, for the sake of mathematical convenience, we set $\mathbf{F}_{\text{BB}} = \frac{1}{\eta}\overline{\mathbf{F}}_{\text{BB}}$ where $\eta \in \mathbb{R}$ represents a normalization factor to satisfy constraint (8). Then, with equation (10), $\|\mathbf{F}_{\text{RF}}\mathbf{F}_{\text{BB}}\|_F^2$ can be expressed as

$$\begin{aligned}\|\mathbf{F}_{\text{RF}}\mathbf{F}_{\text{BB}}\|_F^2 &= \|\frac{1}{\eta}\mathbf{F}_{\text{RFA}}\overline{\mathbf{F}}_{\text{BB}} + \frac{1}{\eta}\mathbf{F}_{\text{L}}\overline{\mathbf{F}}_{\text{BB}}\|_F^2 \\ &= \|\mathbf{F}_{\text{FD}} + \frac{1}{\eta}\mathbf{F}_{\text{L}}\overline{\mathbf{F}}_{\text{BB}}\|_F^2. \end{aligned} \tag{11}$$

Finally, we can rewrite the attenuation loss minimization problem as

$$\text{(P-1)} \quad \min_{\eta,\mathbf{F}_{\text{RFA}},\mathbf{F}_{\text{RF}},\mathbf{F}_{\text{L}},\overline{\mathbf{F}}_{\text{BB}}} \left\|\mathbf{F}_{\text{FD}} + \frac{1}{\eta}\mathbf{F}_{\text{L}}\overline{\mathbf{F}}_{\text{BB}}\right\|_F^2 \tag{12a}$$

$$\text{s.t.} \quad \mathbf{F}_{\text{FD}} = \frac{1}{\eta}\mathbf{F}_{\text{RFA}}\overline{\mathbf{F}}_{\text{BB}}, \tag{12b}$$

$$|\mathbf{F}_{\text{RFA}}^{(i,j)}| \leq \frac{1}{\sqrt{N_{\text{BS}}}}, \ \forall i, j, \tag{12c}$$

$$\mathbf{F}_{\text{RF}}^{(i,j)} = \frac{1}{\sqrt{N_{\text{BS}}}} \exp(j\angle\, \mathbf{F}_{\text{RFA}}^{(i,j)}), \ \forall i, j, \tag{12d}$$

$$\mathbf{F}_{\text{L}} = \mathbf{F}_{\text{RF}} - \mathbf{F}_{\text{RFA}}, \tag{12e}$$

$$\|\mathbf{F}_{\text{RFA}}\mathbf{F}_{\text{BB}}\|_F^2 \leq P_{\text{rad}}, \tag{12f}$$

where (12b) is the constraint for achieving the same SE as the FD and (12d) is the same phase constraint described in (10).

Now, we solve the problem (P-1) by adopting an alternating optimization method that contains a few simple steps. First, for any given initial values of η and $\mathbf{F}_{\text{L}}$, we can determine $\overline{\mathbf{F}}_{\text{BB}}$ by setting the first derivative of (12a) with respect to $\overline{\mathbf{F}}_{\text{BB}}$ to zero as

$$\overline{\mathbf{F}}_{\text{BB}} = -\eta(\mathbf{F}_{\text{L}}^H\mathbf{F}_{\text{L}})^{-1}\mathbf{F}_{\text{L}}^H\mathbf{F}_{\text{FD}}. \tag{13}$$

Note that $\mathbf{F}_{\text{FD}}$ can be predetermined by an existing optimization methods such as the weighted minimum mean square error method [16].

Second, as $\overline{\mathbf{F}}_{\text{BB}}$ is invertible, $\mathbf{F}_{\text{RFA}}$ can be updated as

$$\mathbf{F}_{\text{RFA}} = \eta\mathbf{F}_{\text{FD}}\overline{\mathbf{F}}_{\text{BB}}^{-1}, \tag{14}$$

due to the constraint in (12b) where we have

$$\eta = \frac{1}{\sqrt{N_{\text{BS}}}\max\limits_{i,j}|(\mathbf{F}_{\text{FD}}\overline{\mathbf{F}}_{\text{BB}}^{-1})^{(i,j)}|}, \tag{15}$$

to minimize (12a) while satisfying the condition (12c).

Finally, the RF precoder $\mathbf{F}_{\text{RF}}$ and the attenuator loss matrix $\mathbf{F}_{\text{L}}$ can be acquired from (12d) and (12e), respectively. These steps are repeated until convergence. Due to joint non-convexity of (P-1), N_{G} different initial points are applied and the best solution is selected which minimizes P_{A}. The proposed minimization algorithm for (P-1) is summarized in Algorithm 1.

IV. Simulation Results

In this section, we present simulation results to demonstrate the performance of the proposed HBF architecture and the attenuation loss minimization algorithm. We consider the carrier frequency of 60 GHz for multi-user mmWave systems. We employ a uniform planar array and adopt a mmWave propagation channel model with 8 scattering clusters and 10 propagation paths per each cluster. We set the range of the average azimuth and elevation angles at a BS to 120° and 90°, respectively. Also, the antenna at a UE is assumed to be omni-directional.

Algorithm 1: Attenuation Loss Minimization.

Obtain the FD precoder solution $\mathbf{F}_{\text{FD}}$, and initialize η and $\mathbf{F}_{\text{L}}$
Repeat
  Obtain $\overline{\mathbf{F}}_{\text{BB}}$ from (13) for given η and $\mathbf{F}_{\text{L}}$.
  Update η from (15) for given $\overline{\mathbf{F}}_{\text{BB}}$.
  Obtain $\mathbf{F}_{\text{RFA}}$ from (14) for given η and $\overline{\mathbf{F}}_{\text{BB}}$.
  Obtain $\mathbf{F}_{\text{RF}}$ from (12d).
  Obtain $\mathbf{F}_{\text{L}}$ from (12e).
until convergence

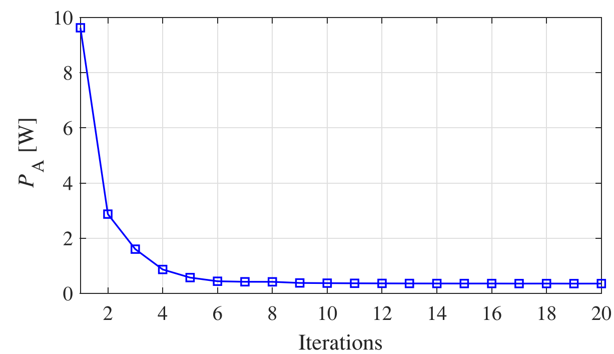

Fig. 2. Convergence of the proposed algorithm.

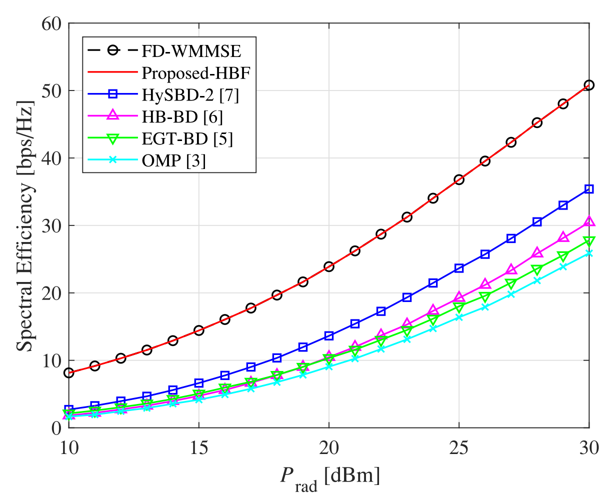

Fig. 3. Average sum-rate comparison with respect to P_{rad} for $K = 4$, $N_{\text{BS}} = 64$, $N_{\text{UE}} = 16$, $M_{\text{BS}} = 8$ and $M_{\text{UE}} = 2$.

The distance between a BS and each UE is fixed to 300 m, and the noise figure is 9 dB.

In Fig. 2, we first examine the convergence of the proposed algorithm for $K = 4$, $N_{\text{BS}} = 64$ and $P_{\text{rad}} = 20$ dBm. It is seen from the figure that the proposed algorithm converges within only a few iterations. We observe that $N_{\text{G}} = 20$ is sufficient to achieve the best performance. The complexity of the proposed algorithm is computed as $\mathcal{O}(N_{\text{G}}N_{\text{i}}M_{\text{BS}}^3) + \mathcal{O}(N_{\text{G}}N_{\text{i}}M_{\text{BS}}^2N_{\text{BS}}) + \mathcal{O}(N_{\text{G}}N_{\text{i}}M_{\text{BS}}N_{\text{BS}}) + \mathcal{O}(N_{\text{G}}N_{\text{i}}M_{\text{BS}}^2) + \mathcal{O}(N_{\text{G}}N_{\text{i}})$, where N_{i} indicates the number of iterations until convergence.

In Fig. 3, we plot the average sum-rate performance of various schemes with respect to the radiated power P_{rad} with $K = 4$, $N_{\text{BS}} =$

Authorized licensed use limited to: Korea University. Downloaded on August 18,2020 at 09:08:21 UTC from IEEE Xplore. Restrictions apply.

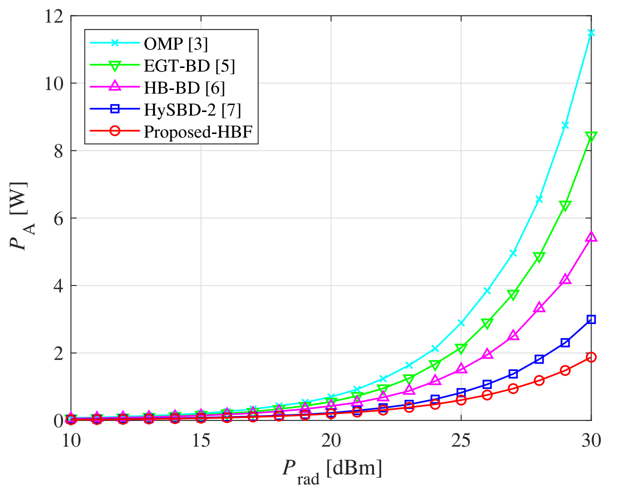

Fig. 4. Average P_{A} with respect to P_{rad} for $N_{\mathrm{BS}} = 64$, $M_{\mathrm{BS}} = 8$ and $N_{\mathrm{G}} = 20$.

64, $N_{\mathrm{UE}} = 16$, $M_{\mathrm{BS}} = 8$ and $M_{\mathrm{UE}} = 2$. We compare our proposed scheme with conventional HBF schemes such as OMP [4], EGT-BD [6], HB-BD [7] and HySBD-2 [8]. Note that the EGT-BD utilizes hybrid block diagonalization (BD) with an equal gain transmission (EGT) method and the HB-BD employs an analog design based on the equivalent baseband channel. The HySBD-2 indicates a joint beamforming scheme utilizing the orthogonalized BB channels by the BD. The OMP here is an extended version of the work [4] to multi-user systems by applying the BD algorithm in a baseband design to manage inter-user interference. The number of RF chains is set to 8 and 64 for the HBF designs including the proposed one and the FD design, respectively. we confirm from the figure that the proposed architecture achieves the optimal FD performance with 8 times less number of RF chains. Also, we can see that the proposed scheme outperforms conventional HBF methods at the same number of RF chains.

Fig. 4 plots the average attenuation loss P_{A} as a function of P_{rad} with $N_{\mathrm{BS}} = 64$, $M_{\mathrm{BS}} = 8$ and $N_{\mathrm{G}} = 20$. Since there is no attenuator in the traditional HBF structure, P_{A} is marked as additional radiation power required to achieve the same performance as the FD scheme. We observe that in the case of $P_{\mathrm{rad}} = 30$ dBm, the proposed scheme achieves a 37.4% gain compared to the HySBD-2 in terms of power loss.

V. Conclusion

In this paper, we have proposed a new HBF structure in which a variable attenuator is implemented at each phase shifter. We have shown that our HBF structure guarantees the optimal performance of the FD structure with the reduced number of RF chains. Also, we have provided an effective HBF design algorithm which minimizes the attenuation loss in the proposed architecture. Simulation results have confirmed that the proposed algorithm requires much lower power compared to other conventional HBF schemes. A more practical scenario with imperfect channel-state information would be an important future work.

References

[1] J. G. Andrews *et al.*, "What will 5G be?" *IEEE J. Sel. Areas Commun.*, vol. 32, no. 6, pp. 1065–1082, Jun. 2014.

[2] M. Baianifar, S. M. Razavizadeh, H. Akhlaghpasand, and I. Lee, "Energy efficiency maximization in mmWave wireless networks with 3D beamforming," *J. Commun. Netw.*, vol. 21, pp. 125–135, Apr. 2019.

[3] A. F. Molisch *et al.*, "Hybrid beamforming for massive MIMO: A survey," *IEEE Commun. Mag.*, vol. 55, no. 9, pp. 134–141, Sep. 2017.

[4] O. E. Ayach, S. Rajagopal, S. Abu-Surra, Z. Pi, and R. W. Heath, "Spatially sparse precoding in millimeter wave MIMO systems," *IEEE Trans. Wireless Commun.*, vol. 13, no. 3, pp. 1499–1513, Mar. 2014.

[5] T. Oh, C. Song, S. Jang, and I. Lee, "Hybrid analogdigital filter designs for mmwave multipair two-way relaying systems," *IEEE Trans. Veh. Technol.*, vol. 67, no. 8, pp. 7841–7845, Aug. 2018.

[6] W. Ni and X. Dong, "Hybrid block diagonalization for massive multiuser MIMO systems," *IEEE Trans. Commun.*, vol. 64, no. 1, pp. 201–211, Jan. 2016.

[7] C. Hu, J. Liu, X. Liao, Y. Liu, and J. Wang, "A novel equivalent baseband channel of hybrid beamforming in massive multiuser MIMO systems," *IEEE Commun. Lett*, vol. 22, no. 4, pp. 764–767, Apr. 2018.

[8] X. Wu, D. Liu, and F. Yin, "Hybrid beamforming for multi-user massive MIMO systems," *IEEE Trans. Commun.*, vol. 66, no. 9, pp. 3879–3891, Sep. 2018.

[9] T. Oh, C. Song, J. Jung, M. Ahn, J. Kim, and I. Lee, "A new RF beam training method and asymptotic performance analysis for multi-user millimeter wave systems," *IEEE Access*, vol. 6, pp. 48 125–48 135, Aug. 2018.

[10] J. Kim, S.-H. Park, O. Simeone, I. Lee, and S. Shamai, "Joint design of fronthauling and hybrid beamforming for downlink C-RAN systems," *IEEE Trans. Commun.*, vol. 67, no. 6, pp. 4423–4434, Jun. 2019.

[11] X. Zhang, A. Molisch, and S.-Y. Kung, "Variable-phase-shift-based RF-baseband codesign for MIMO antenna selection," *IEEE Trans. Signal Process.*, vol. 53, no. 11, pp. 4091–4103, Nov. 2005.

[12] H. Mohammadnezhad, R. Abedi, and P. Heydari, "A millimeter-wave partially overlapped beamforming-MIMO receiver: Theory, design, and implementation," *IEEE Trans. Microw. Theory Techn.*, vol. 67, no. 5, pp. 1924–1936, May 2019.

[13] M. R. Castellanos, V. Raghavan, J. H. Ryu, O. H. Koymen, J. Li, D. J. Love, and B. Peleato, "Channel-reconstruction-based hybrid precoding for millimeter-wave multi-user MIMO systems," *IEEE J. Sel. Topics Signal Process.*, vol. 12, no. 2, pp. 383–398, May 2018.

[14] H. Dogan, R. G. Meyer, and A. M. Niknejad, "Analysis and design of RF CMOS attenuators," *IEEE J. Solid-State Circuits*, vol. 43, no. 10, pp. 2269–2283, Oct. 2008.

[15] J. Bae, J. Lee, and C. Nguyen, "A 10-67-GHz CMOS dual-functioin switching attenuator with improved flatness and large attenuation range," *IEEE Trans. Microw. Theory Techn.*, vol. 61, no. 12, pp. 4118–4129, Dec. 2013.

[16] Q. Shi, M. Razaviyayn, Z.-Q. Luo, and C. He, "An iteratively weighted MMSE approach to distributed sum-utility maximization for a MIMO interfering broadcast channel," *IEEE Trans. Signal Process.*, vol. 59, no. 9, pp. 4331–4340, Sep. 2011.

Authorized licensed use limited to: Korea University. Downloaded on August 18,2020 at 09:08:21 UTC from IEEE Xplore. Restrictions apply.